

Perpendicularly Oriented Polycrystalline BaFe_{11.1}Sc_{0.9}O₁₉ Hexaferrite with Narrow FMR Linewidths

Yajie Chen,^{*,†} Michael J. Nedoroscik, Anton L. Geiler, Carmine Vittoria, and Vincent G. Harris

Department of Electrical and Computer Engineering, and the Center for Microwave Magnetic Materials and Integrated Circuits, Northeastern University, Boston, Massachusetts 02115

We demonstrate low ferromagnetic resonance (FMR) linewidths and high remanence magnetization in polycrystalline M-type Sc-doped Ba ferrites having anisotropy fields of ~8 kOe and perpendicular orientation of the spontaneous magnetization vector. This is a result of applying a unique processing technique that makes use of a polymer network-assisted alignment of hexaferrite particles in high magnetic fields. The resulting compacts exhibit high squareness ($M_r/M_s \sim 92\%$) and low FMR linewidths (~530 Oe) at X-band and Ka-band. This represents an ~74% decrease in linewidth compared with previous reports for polycrystalline BaM ferrites using conventional processes. We also have detailed origins of the FMR linewidth broadenings in terms of some important theoretical models. These materials have potential for use in low frequency self-biased microwave/millimeter devices such as circulators and isolators.

I. Introduction

ALTHOUGH hexaferrites have been widely used in the electronics industry for more than a half of century, there has been an increasing interest in new opportunities for these materials in modern electronic devices,^{1,2} microwave communication,³ and nanotechnology applications.⁴ The hexagonal ferrite with M-type structure, BaFe₁₂O₁₉ (or BaM), features high saturation magnetization and a uniaxial magnetocrystalline anisotropy field that acts as an effective built-in magnetic field. As such, with appropriate chemical substitutions, ferromagnetic resonance (FMR) extends from microwave to millimeter wave frequencies allowing their application in such devices as isolators, filters, phase shifters, and circulators. A key component of radar electronics is the circulator, which usually includes a permanent magnet to provide the biasing magnetic field required for operation. These devices are three-dimensional constructs that are often bulky and costly to fabricate. It is anticipated that the next generation of magnetic microwave devices will be planar, self-biased and low-loss, and will operate well beyond the performance metrics of today's devices. Self-biasing is an important property that eliminates the need for the permanent magnet and reduces the size, weight, and assembly cost of microwave devices.⁵

In order to achieve these goals, ferrite materials must possess high saturation magnetization ($4\pi M_s$), high remanent magnetization ($4\pi M_r$), adjustable magnetic anisotropy fields (H_a), low FMR linewidths (ΔH), and, for many applications, have the easy axis of magnetization perpendicular to the substrate or the plane of the device. In physical terms, the materials should range in thickness between 100 and 500 μm , contain low levels of

porosity, which is responsible for added FMR linewidths, and be of a pure and high crystal quality phase.⁶

Since 1989, researchers at the MIT-Lincoln Laboratory⁷ and Northeastern University^{8,9} have demonstrated prototypes of self-biased microwave circulators at Ka band. However, large microwave losses have severely hindered the realization of practical devices. Therefore, the ability to fabricate low-loss ferrite materials having high remanence magnetization is a pivotal step in realizing planar devices that can be commercialized. Because of the large prospective markets in commercial and military communications and radar, the potential for low-frequency, low-field, and low-loss planar microwave devices (i.e., FMR frequencies from 1 to 40 GHz) has received great interest.¹⁰ The hexaferrite may become one of the key components in self-biased devices and integrated microwave circuits due to its adjustable uniaxial magnetic anisotropy field. The biggest challenges remain the stabilization of a high remanent magnetization, low microwave losses, and tunable anisotropy fields. Anisotropy fields of <10 kOe can be achieved with the substitution of scandium, indium, etc. for Fe in Ba hexaferrites.^{11–14} This has been a longstanding challenge, whose solution will have a wide-ranging impact on the field of low-frequency microwave magnetic devices working at 1–20 GHz.

In this paper, we report important progress in the synthesis of BaFe_{11.1}Sc_{0.9}O₁₉ hexaferrite materials, where Sc doping is responsible for reducing the anisotropy field and FMR frequency. This is a result of a processing technique that utilizes a polymer network-assisted-alignment process (PNAAP), whereupon the low H_a ferrite particles were aligned in magnetic fields. Besides structure, magnetic, and microwave property measurements, some theoretical estimates of the FMR linewidth for textured polycrystalline materials are presented.

II. Experimental Procedure

The starting powders were prepared by conventional ceramic processing of BaCO₃, Fe₂O₃, and Sc₂O₃ to form a pure phase of BaFe_{11.1}Sc_{0.9}O₁₉. PNAAP was used to achieve high magnetic orientation of ferrite particles. In this methodology, a slurry typically consists of a 60–70 wt% hexaferrite particle and a 30–40 wt% acrylamide polymer solution that comprises acrylamide monomer, methylenebisacrylamide monomer, ammonium persulfate and tetramethylethylenediamine. The slurry is subsequently cast into a plastic mold. The resulting cylinder or disk compact is subjected to a large magnetic field (10–90 kOe) aligned along the perpendicular axis of the compact during polymerization at room temperature for 1–10 h. This alignment forces the c-axes of the hexaferrite particles, and subsequently the magnetization, to align along the direction of the applied magnetic field. The polymer matrix was removed by a burnout performed at 650°C and subsequently the green body was uniaxially pressed at 10 MPa. Finally, the ferrite compact was sintered at 1050–1150°C.

The samples were characterized in terms of their structural, magnetic, and microwave properties. The degree of crystallographic orientation was obtained from Philips X'pert PRO X-ray diffraction (XRD, the Netherlands) measurements using

P. Joy—contributing editor

Manuscript No. 24370. Received March 3, 2008; approved June 4, 2008.

^{*}Member, The American Ceramic Society

The work was financially supported by the Office of Naval Research under Grant No. N00014-05-1-0349 and the Army Research Office under Grant No. 52779-MS-DRP.

[†]Author to whom correspondence should be addressed. e-mail: y.chen@neu.edu

a $CuK\alpha$ radiation source. The morphology was examined using a Hitachi S-4800 (Japan) ultrahigh-resolution scanning electron microscope (SEM). Static magnetic properties were measured using a Lakeshore vibrating sample magnetometer (VSM, Westerville, OH) and a Quantum Design Physical Property Measurement System (San Diego, CA) at room temperature, and microwave magnetic properties were characterized by the FMR measurements using a shorted waveguide at 26.5–40 GHz. In the FMR measurements, the external magnetic field was applied perpendicular to the plane, and swept. The frequency was fixed during the field sweep. Because the magnetic easy axis was perpendicular to the film plane, we applied the external magnetic field H_0 parallel to the easy direction, i.e. perpendicular to the film plane. Thus, the microwave magnetic field h was applied in the plane of the sample. At $f = 9.65$ GHz (X-band), the FMR linewidth of the sample was measured using a field sweep FMR/electron paramagnetic resonance, FMR/EPR, facility with both dc magnetic field and microwave excitation field in the plane of the samples. In addition, the dielectric loss was determined to be $\tan(\delta) < 0.01$ by transmission/reflection method at K-band (18–26.5 GHz).¹⁵

III. Results and Discussion

(1) XRD Spectrum

A representative XRD pattern of textured Sc-doped BaM ferrite is shown in Fig. 1. All diffraction features have been indexed to space group $P6_3/mmc$ (published pattern: ICDD-#43-0002), corresponding to the magnetoplumbite structure. Because the magnetic easy axis determines the preferred orientation of magnetization, the Lotgering method was used to quantify the degree of crystallographic alignment of the sample. X-ray θ - 2θ diffraction spectra using $CuK\alpha$ radiation were taken from polished surfaces perpendicular to the anticipated alignment axis. The texture fraction of the (00l) plane was calculated using the Lotgering factor by the following equation¹⁶:

$$f = \frac{P - P_0}{1 - P_0} \quad (1)$$

where $P = \frac{\sum I_{(00l)}}{\sum I_{(hkl)}}$ for oriented samples, and $P_0 = \frac{\sum I_{0(00l)}}{\sum I_{0(hkl)}}$ for the standard random powder using the published diffraction file ICDD, #43-0002. Diffraction peaks in the 2θ range of 20° – 100° were used for the calculation. The estimated texture fraction of the (00l)-plane in the aligned sample is $f = 0.73$. In order to achieve a strong crystal texture and in turn high remanence, the average grain size must be less than or close to the single domain size. However, a low anisotropy field, H_a , may be responsible for a small critical size, whereas a high Lotgering factor is generally associated with the loss of small grain size and high anisotropy field.^{17,18} Therefore, an optimal process requires a reasonable tradeoff of preferred orientation and magnetic properties. In this

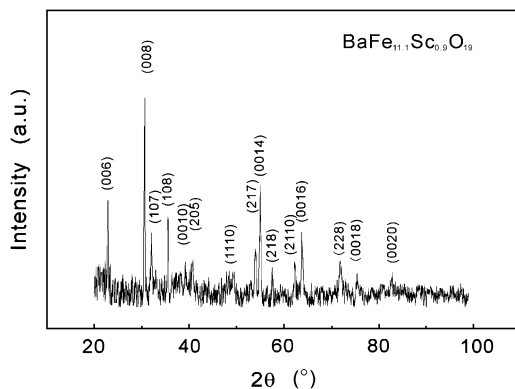


Fig. 1. X-ray diffraction patterns of an oriented $BaFe_{11.1}Sc_{0.9}O_{19}$ compact after sintering at a temperature of 1150°C for 4 h.

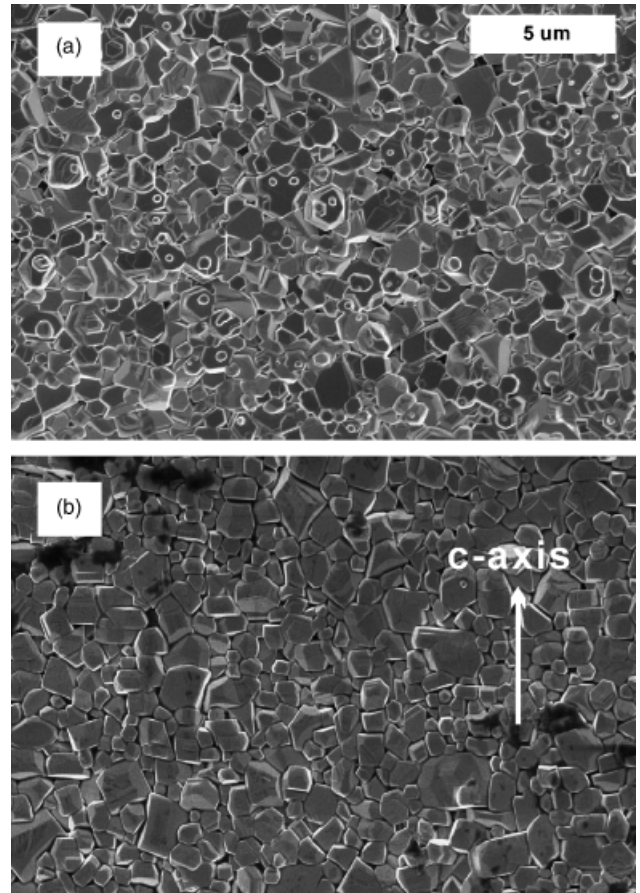


Fig. 2. Scanning electron micrographs of Sc-doped BaM ferrite: (a) surface, and (b) cross section of the compact after sintering at 1150°C for 4 h.

case, the morphology and structure characterizations clearly indicated a strong crystal texture of c -axis grains normal to the sample plane. Furthermore, to obtain high remanent magnetization and hysteresis loop squareness, it was crucial to control the distribution and size of the ferrite grains.^{19,20}

(2) SEM Analysis

The magnetic and crystallographic properties of ferrite materials are extremely sensitive to the preparation processing, such as sintering conditions. Correlation of microstructure and magnetic property can be clarified by means of SEM analysis. Figures 2(a) and (b) present SEM images of the surface and cross section of the Sc-doped BaM ferrite, respectively. Figure 2(a) reveals that the material has grain sizes ranging from 0.4 to $1.8 \mu\text{m}$ and an average grain size of $0.8 \pm 5\% \mu\text{m}$, whereas the estimated single domain critical size ranges from 0.5 to $1.0 \mu\text{m}$. Thus, it is suggested that most of the grains are of the spin configuration of magnetic single domain, which is of significant importance in the preparation of materials with high remanence. In Fig. 2(b), it is observed that the majority of the grains demonstrate a preferred alignment, along with the hexagonal crystallographic c -axis, perpendicular to the sample plane. At the same time, some misalignment of grains can be seen as well, which is consistent with the moderate Lotgering factor (~ 0.72). Moreover, the density was measured to be $92 \pm 2\%$ of the theoretical density, which means that the sample still contains pores. Some small pores (100–300 nm) are visible in Fig. 2. These pores may result in a broadening of FMR linewidths, i.e. an extrinsic broadening. This will be discussed more in Section III(4).

(3) Magnetic Hysteresis Measurements

In order to characterize the relation between microstructure and magnetic properties in the ferrite, dc magnetic hysteresis was

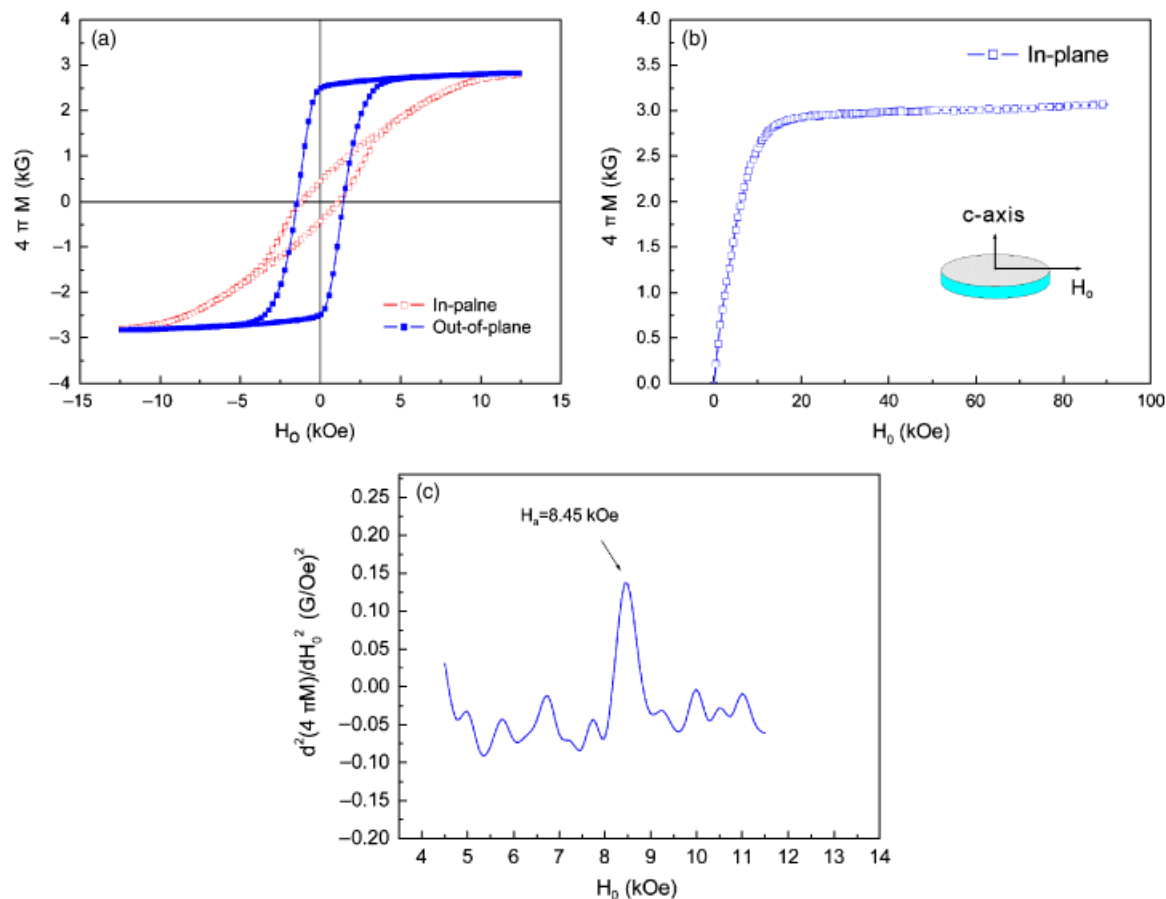


Fig. 3. (a) Magnetic hysteresis loops with applied magnetic field aligned in the sample plane (hollow square) and perpendicular to the sample plane (solid square), (b) virgin magnetization curve with magnetic field perpendicular to hexagonal crystallographic c -axis, and (c) the second derivative [$d^2(4\pi M)/dH_0^2$] of the virgin magnetization curve along with hard axis for the BaFe_{11.1}Sc_{0.9}O₁₉ compact after optimal processing (see text).

measured using VSM. Figure 3 shows representative static magnetic hysteresis loops (M versus H) for the Sc-doped BaM sample. It is clear that the sample has obvious differences in hysteresis loops when an external field is applied in the sample plane and out of plane. Hence, this material has an anisotropic magnetic behavior that is due to a preferred orientation of grains. In Fig. 3(a), the hysteresis loop with a high remanent magnetization ($M_r \sim 2570$ G) corresponds to the out-of-plane orientation. This is a very important result in that it demonstrates two important properties of the aligned ferrite samples. Firstly, the magnetization prefers the direction normal to the sample plane, which is in agreement with the XRD results. In this case, the magnetization was $4\pi M = 2.8 \pm 0.2$ kG at a field of 12.5 kOe, with a coercivity of 1.43 kOe for the out-of-plane measurement. Secondly, upon removal of the applied field, the sample retained 92% of the saturation magnetization (i.e., remanent magnetization). The remanent magnetization is a key parameter of the ferrite material that may enable self-biased microwave devices, such as circulators, to work with no biasing magnets. This development will help solve a significant problem that has been hampering advancement in both military technology and modern commercial communications for the past few decades.²¹

Figure 3(b) presents a virgin magnetization curve for the same sample, where an external field, H_0 , (up to 90 kOe) is applied perpendicular to the hexagonal crystallographic c -axis. Here, the saturation magnetization ($4\pi M_s$) obtained was 3.0 kG at $H = 90$ kOe. Note, a kink in the magnetization curve reflects the degree of grain orientation. Because of some misalignment of grains, the kink evolves slowly rather than abruptly. In order to determine a magnetocrystalline anisotropy field for the oriented ferrite, a singular point detection method²² was applied to estimate the present sample. In this method, the maximum in the

second derivative (d^2M/dH_0^2) of the virgin magnetization curve along the hard axis corresponds to the anisotropy field. This technique has been applied to measure the anisotropy field in oriented polycrystalline samples.²³ From Fig. 3(c), it is clear that the second derivative (d^2M/dH_0^2) exhibits a peak at $H_0 = 8.45$ kOe corresponding to the anisotropy field, H_a , once corrected for the demagnetizing field. Because the measured sample is a thin disk ($\Phi 3$ mm \times 0.5 mm), the effect of the demagnetizing field is negligible. The results are comparable to values obtained from FMR measurements that will be discussed in Section III(4).

Furthermore, a magnetocrystalline anisotropy constant can be calculated in terms of the basic equation, $H_a = 2K_u/M_s$. Thus, we obtain $K_u = 1.01 \times 10^6$ erg/cm³ for BaFe_{11.1}Sc_{0.9}O₁₉, which is in accord with Röschmann's¹² results for Sc-doped BaM single crystals. Previous experiments^{12,24} also indicated the ability to alter the anisotropy fields that can be modified by the scandium amount. These results are of significance in the selection of the compositions that enable the adjustment of the FMR frequency in hexaferrite materials.

(4) FMR Measurements

FMR measurements at Ka band were performed with an applied field perpendicular to the sample plane (Fig. 4). The measured sample had the dimensions of 2.5 mm \times 2.5 mm \times 0.2 mm ($W \times L \times T$). Here, the FMR condition is given as follows²⁵:

$$f = \gamma'(H_0 + H_a - N_z M) \quad (2)$$

where γ' is the gyromagnetic ratio ($\gamma' = 1.4 \times 10^6 \times g$), and g is the Lande factor. Figure 5 depicts the correlation between the FMR absorption as the power derivative and external field over

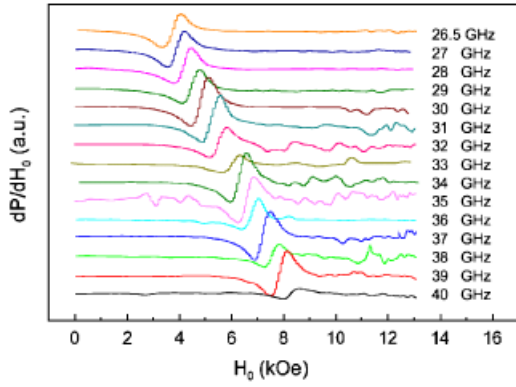


Fig. 4. Correlation between ferromagnetic resonance absorption derivative and external field at the frequency range from 26.5 to 40 GHz. The external field is parallel to the hexagonal crystallographic c -axis, and perpendicular to the sample plane.

the frequency range of 26.5–40 GHz. The external field is aligned parallel to the hexagonal crystallographic c -axis, and perpendicular to the sample plane. Clearly, the FMR peak can be tuned by an external field. Figure 5 displays the FMR frequency as a function of the external magnetic field, and subsequently, the g -factor was extracted to be 2.08 ± 0.03 . It is noted that the zero field FMR frequency is 15.6 ± 0.2 GHz, as extrapolated from the linear fit to Eq. (2) ($f = 2.92H_0 + 15.6$). More importantly, this ferrite exhibits low FMR linewidths (i.e., $\Delta H = 530$ – 690 Oe) over a broad frequency range (26.5–40 GHz), as depicted in Fig. 6. As a result of FMR measurements, an average linewidth is approximately 600 Oe. These results represent the lowest linewidth observed in polycrystalline Sc-doped hexaferrites. Commercially available barium ferrites typically have ΔH values of ~ 2000 Oe.^{26,27} This represents an $\sim 74\%$ improvement in this critical parameter. The measured FMR linewidths, ~ 600 Oe, are believed to satisfactorily address most requirements of microwave devices. However, it is assumed that the FMR linewidths can be further narrowed by reducing nonuniformity contributions including porosity, misalignment, roughness, etc.²⁸

At X-band ($f = 9.65$ GHz), FMR measurements were carried out using a microwave cavity excited in a TE_{102} mode, where the external field was aligned in the plane of the sample. The in-plane FMR measurement revealed two FMR frequencies at different external fields, which corresponded to linewidths of 550 and 830 Oe, respectively, as presented in Fig. 7. Note that the two resonance fields lie somewhat above and below the anisotropy field, $H_a = 7.86 \pm 0.20$ kOe, obtained from FMR measurements. This value is very close to the $H_a = 8.45$ kOe derived from the second derivative of the virgin magnetization along the magnetic hard axis. As a result of the in-plane FMR measure-

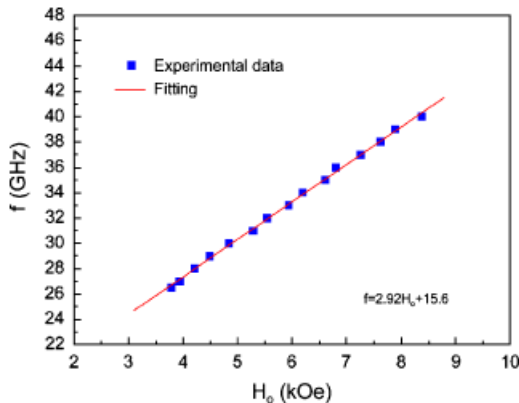


Fig. 5. Field dependence of the ferromagnetic resonance frequency for $BaFe_{11.1}Sc_{0.9}O_{19}$ at Ka frequency band (26.5–40 GHz).

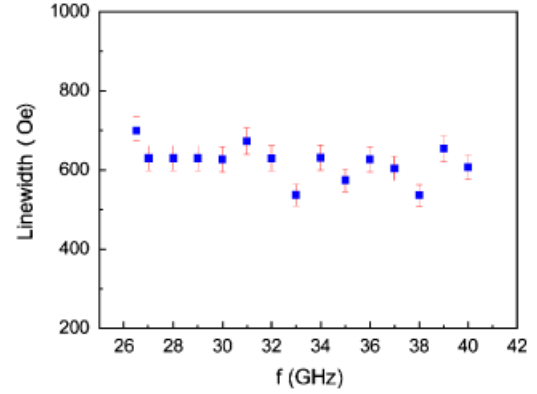


Fig. 6. Frequency dependence of ferromagnetic resonance linewidths for $BaFe_{11.1}Sc_{0.9}O_{19}$ sample at Ka frequency band (26.5–40 GHz).

ment, the observed FMR lines are completely consistent with the theoretical prediction,²⁹ as presented in the inset of Fig. 7.

Broadening of the FMR linewidths from extrinsic sources are indeed inevitable for polycrystalline ferrites. This may present a challenge to realizing low-loss, high-performance devices. In order to find material solutions having narrow linewidths, it is necessary to estimate contributions to the total linewidth for these materials. In general, the total linewidth is attributed to three major contributions,

$$\Delta H = \Delta H_i + \Delta H_a + \Delta H_p \quad (2')$$

where ΔH_i , ΔH_a , and ΔH_p represent intrinsic, random anisotropy field, and porosity, respectively. Clearly, the latter two terms represent extrinsic contributions present in our samples. Spark conducted a detailed calculation of the scattering linewidth due to pores:^{30,31}

$$\Delta H_p = \frac{\pi^2 \omega P M_s}{2\gamma H_0} \frac{(3 \cos^2 \theta_u - 1)^2 + 1.6}{\cos \theta_u} \quad (3)$$

where P is the porosity, ω is the angular frequency, γ the gyromagnetic ratio, H_0 the internal magnetic field, and θ_u is the spin wave angle between the wave vector and the internal field for the uniform mode. Because of $\frac{1}{3} < \cos^2 \theta_u < 1$ for nonspherical voids,³² the estimate shows the porosity contribution to line-

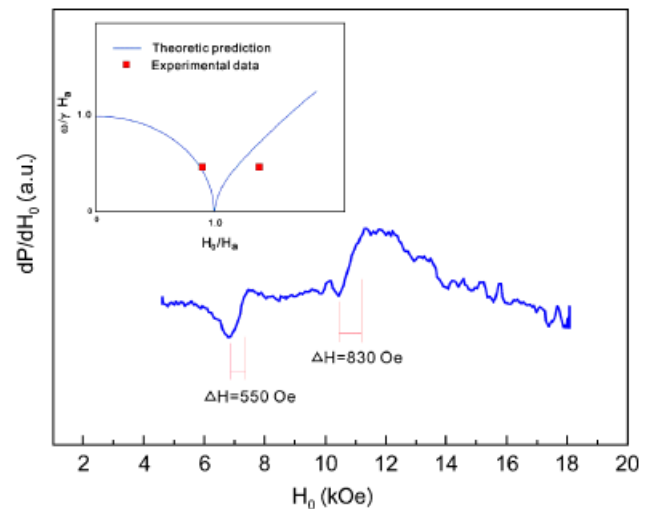


Fig. 7. Variation of ferromagnetic resonance absorption derivative with field at $f = 9.65$ GHz for a $BaFe_{11.1}Sc_{0.9}O_{19}$ sample. Data are collected with the applied field oriented in the sample plane, perpendicular to the crystallographic c -axis. The inset presents theoretical predictions and experimental data for the ferromagnetic resonance measurements.

width ranging from 440 to 900 Oe. The lower limit is very close to the results of 340–420 Oe, derived from Schlöemann's calculation,^{33,34}

$$\Delta H_p = 1.5(4\pi M_s)P \quad (4)$$

Both Eqs. (3) and (4) predict an approximate linewidth contribution of 400 Oe for the case of Sc-doped BaM. Note, our estimate indicates that a random orientation of grains results in a broadening of the linewidth, $\Delta H_a = 32$ Oe ($\Delta H_a = 1.08J \frac{H_a^2}{4\pi M}$, here $J = 1.3$),^{35,36} whereas the intrinsic linewidth of this material (Sc ion number = 1) is about $\Delta H_i = 50$ Oe.¹² The total estimates compare reasonably with the experimental results of $\Delta H_{\text{meas}} = 500\text{--}700$ Oe. Dionne³⁷ also reported linewidth contributions from porosity in single crystals that yielded a coefficient of 0.64 in Eq. (4), less than half of Schlöemann's original estimate for polycrystals. From this, we conclude that the porosity indeed contributes to the broadening of linewidths for polycrystalline ferrites, and an increase in density is expected to narrow the extrinsic linewidth due to the annihilation of pores.³⁸ The reduction in pores may be realized by further growth of the grains at higher sintering temperatures. However, such a strategy is not available for the present hexaferrite, which requires grain sizes to be approximately equal to the single domain size needed to obtain high remanent magnetization and hysteresis loop squareness. Therefore, promising solutions in densification include (1) a final sintering carried out under a hot-isotropic pressure³⁹ and (2) the use of a cold-isotropic press⁴⁰ to press green bodies before sintering. Because both the techniques feature an isotropic pressure, they will likely not result in significant loss of grain alignment in the highly oriented green body.

IV. Conclusion

In summary, we have provided details of a processing scheme in which a polymer network assisted the alignment of hexaferrite particles in high magnetic fields resulting in a highly dense Sc-doped Ba hexaferrite compact. These materials offer low FMR linewidths (500–600 Oe) at X-band and Ka-band and high remanent magnetization ($M_r/M_s \sim 92\%$) and should be suitable for applications in low-frequency microwave devices (1–20 GHz). The ferrite compacts have good mechanical properties and adjustable thicknesses ranging from 100 to 500 μm , which can be sufficient to allow the development of planar microwave circulators. Also, the preparation process can be readily transferable to other hexaferrites, such as In/Sc-doped Ba/Sr hexaferrites.

Reference

- ¹W. Eerenstein, N. D. Mathur, and J. F. Scott, "Multiferroic and Magneto-electric Materials," *Nature*, **442**, 759–65 (2006).
- ²T. Kimura, G. Lawes, and A. P. Ramirez, "Electric Polarization Rotation in a Hexaferrite with Long-Wavelength Magnetic Structures," *Phys. Rev. Lett.*, **94**, 137201 (2005).
- ³J. Douglas Adam, L. E. Davis, G. F. Dionne, E. F. Schlöemann, and S. N. Stitzer, "Ferrite Devices and Materials," *IEEE Trans. Microwave Theory Tech.*, **50**, 721–37 (2002).
- ⁴I. P. Parkin, G. Elwin, L. F. Barquin, Q. I. Bui, Q. A. Pankhurst, A. K. Komarov, and Y. G. Morozov, "Self-Propagating High Temperature Synthesis of Hexagonal Ferrites $M\text{Fe}_{12}\text{O}_{19}$ ($M = \text{Sr}, \text{Ba}$)," *Adv. Mater.*, **9**, 643–5 (1997).
- ⁵V. G. Harris, Z. Chen, Y. Chen, A. Yang, S. Yoon, A. Gieler, T. Sakai, K. Ziemer, N. Sun, and C. Vittoria, "Ba-Hexaferrite Films for Next Generation Microwave Devices," *J. Appl. Phys.*, **99**, 08M911 (2006).
- ⁶Y. Chen, T. Sakai, T. Chen, S. D. Yoon, A. L. Geiler, C. Vittoria, and V. G. Harris, "Oriented Barium Hexaferrite Thick Films with Narrow Ferromagnetic Resonance Linewidth," *Appl. Phys. Lett.*, **88**, 062516 (2006).
- ⁷J. A. Weiss, N. G. Watson, and G. F. Dionne, "New Uniaxial-Ferrite Millimeter-Wave Junction Circulators," *IEEE MTT-S Digest*, 145 (1989).
- ⁸N. Zeina, H. How, C. Vittoria, and R. West, "Self-Biasing Circulators Operating at Ka-Band Utilizing M-type Hexagonal Ferrites," *IEEE Trans. Magn.*, **28**, 3219–21 (1992).

- ⁹S. A. Oliver, P. Shi, W. Hu, H. How, S. W. McKnight, N. E. McGruer, P. M. Zavracky, and C. Vittoria, "Integrated Self-Biased Hexaferrite Microstrip Circulators for Millimeter-Wavelength Applications," *IEEE Trans. Microwave Theory Tech.*, **49**, 385–7 (2001).
- ¹⁰E. Schlöemann, "Advances in Ferrite Microwave Materials and Devices," *J. Magn. Magn. Mater.*, **209**, 15–20 (2000).
- ¹¹G. F. Dionne and J. F. Fitzgerald, "Magnetic Hysteresis Properties of $\text{BaFe}_{12-x}\text{In}_x\text{O}_{19}$ Ceramic Ferrites with c -Axis Oriented Grains," *J. Appl. Phys.*, **70**, 6140–2 (1991).
- ¹²P. Röschmann, M. Lemke, W. Tolksdorf, and F. Welz, "Anisotropy Fields and FMR Linewidth in Single-Crystal Al, Ga and Sc Substituted Hexagonal Ferrites with M Structure," *Mater. Res. Bull.*, **19**, 385–90 (1984).
- ¹³L. M. Silber, E. Tsantes, and W. D. Wilber, "Temperature Dependence of Ferromagnetic Resonance Linewidth in Pure and Substituted Barium Ferrite," *J. Magn. Magn. Mater.*, **54–57**, 1141–2 (1986).
- ¹⁴W. D. Wilber, L. M. Silber, and A. Tauber, "Hexagonal Ferrites for Millimeter-Wave Control Devices," *Res. Dev. Tech. Rep. SLCET-TR*, **87**, 4 (1987).
- ¹⁵J. Baker-Jarvis, E. J. Vanzura, and W. A. Kissick, "Improved Technique for Determining Complex Permittivity with the Transmission/Reflection Method," *IEEE Trans. Microwave Theory Tech.*, **38**, 1096–103 (1990).
- ¹⁶F. K. Lotgering, "Topotactical Reactions with Ferromagnetic Oxides Having Hexagonal Crystal Structure-I," *J. Inorg. Nucl. Chem.*, **9**, 113–23 (1959).
- ¹⁷M. M. Seabaugh, I. H. Kersch, and G. L. Messing, "Texture Development by Templated Grain Growth in Liquid-Phase-Sintered α -Alumina," *J. Am. Ceram. Soc.*, **80**, 1181–8 (1997).
- ¹⁸D. R. Franklin, A. J. Pointon, and R. C. L. Jenkins, "Resonance Linewidths and Crystallite Alignment in Oriented Samples of Polycrystalline Barium Hexaferrite," *J. Phys. D: Appl. Phys.*, **29**, 1268–73 (1996).
- ¹⁹J. E. Knowles, "Some Observations of Bitter Patterns on Polycrystalline 'Square Loop' Ferrites, and a Theoretical Explanation of the Loop Shape and Pulse Characteristics of the Material," *Proc. Phys. Soc.*, **75**, 885–97 (1959).
- ²⁰E. A. Schwabe and D. A. Campbell, "Influence of Grain Size on Square-Loop Properties of Lithium Ferrites," *J. Appl. Phys.*, **34**, 1251–3 (1963).
- ²¹V. G. Harris, A. L. Geiler, Y. Chen, S. D. Yoon, M. Wu, A. Yang, Z. Chen, P. He, P. V. Parimi, X. Zuo, C. E. Patton, M. Abe, O. Acher, and C. Vittoria, "Recent Advances in the Processing and Applications of Microwave Ferrites," *J. Magn. Magn. Mater.*, (2008) (in press).
- ²²H. Nishio, H. Taguchi, S. Hashimoto, K. Yajima, A. Fukuno, and H. A. Yamamoto, "Comparison of Magnetic Anisotropy Constants and Anisotropy Fields of Permanent Magnets Determined by Various Measuring Methods," *J. Phys. D: Appl. Phys.*, **29**, 2240–5 (1996).
- ²³G. Asti and S. Rinaldi, "Singular Points in the Magnetization Curve of a Polycrystalline Ferromagnet," *J. Appl. Phys.*, **45**, 3600–10 (1974).
- ²⁴T. Sakai, Y. Chen, C. N. Chinnsamy, C. Vittoria, and V. G. Harris, "Textured Sc-Doped Barium Ferrite Compacts for Microwave Applications Below 20 GHz," *IEEE Trans. Magn.*, **42**, 3353–5 (2006).
- ²⁵C. Vittoria, *Microwave Properties of Magnetic Films*. World Scientific, Singapore, 1993.
- ²⁶Y. Akaiwa and T. Okazaki, "An Application of a Hexagonal Ferrite to a Millimeter-Wave Y Circulator," *IEEE Trans. Magn.*, **10**, 374–8 (1974).
- ²⁷D. J. De Bitetto, "Anisotropy Field in Hexagonal Ferromagnetic Oxides by Ferromagnetic Resonance," *J. Appl. Phys.*, **35**, 3482–7 (1964).
- ²⁸U. Hoeppe and H. Benner, "Microstructure-Related Relaxation and Spin-Wave Linewidth in Polycrystalline Ferromagnets," *Phys. Rev. B*, **71**, 144403 (2005).
- ²⁹F. J. Rachford, P. Lubitz, and C. Vittoria, "Microwave Resonance and Propagation in Nonsaturated Ferromagnetic Media I. Magnetic Resonance in Single Crystal Ferrite Platelets," *J. Appl. Phys.*, **53**, 8940–51 (1982).
- ³⁰C. L. Patton, "A Review of Microwave Relaxation in Polycrystalline Ferrites," *Intermag Conference*, 433–9, Kyoto, Japan, 1972.
- ³¹M. Sparks, "Ferromagnetic Resonance Porosity Linewidth Theory in Polycrystalline Insulators," *J. Appl. Phys.*, **36**, 1570–3 (1965).
- ³²A. S. Risley and H. E. Bussey, "Ferromagnetic Resonance Relaxation, Wide Spin-Wave Coverage by Ellipsoids," *J. Appl. Phys.*, **35**, 896–7 (1964).
- ³³E. Schlöemann, "The Microwave Susceptibility of Polycrystalline Ferrites in Strong dc Fields and the Influence of Nonmagnetic Inclusions on the Microwave Susceptibility," *Proc. Conf. Magn. Mater. AIEE Spec. Pub T-91*, 600 (1956).
- ³⁴E. Schlöemann, "Properties of Magnetic Materials with a Nonuniform Saturation Magnetization. I. General Theory and Calculation of the Static Magnetization," *J. Appl. Phys.*, **38**, 5027–34 (1967).
- ³⁵P. E. Seiden and J. G. Grunberg, "Ferromagnetic Resonance Linewidth in Dense Polycrystalline Ferrites," *J. Appl. Phys.*, **34**, 1696–8 (1963).
- ³⁶S. Geschwind and A. M. Clogston, "Narrowing Effect of Dipole Forces on Inhomogeneously Broadened Lines," *Phys. Rev.*, **108**, 49–53 (1957).
- ³⁷G. F. Dionne, "Effect of Porosity on Ferromagnetic Resonance Linewidths," *Mater. Res. Bull.*, **5**, 939–46 (1970).
- ³⁸Y. Chen, T. Sakai, T. Chen, S. Yoon, C. Vittoria, and V. G. Harris, "Screen Printed Thick Self-Biased, Low-Loss, Barium Hexaferrite Films by Hot-Press Sintering," *J. Appl. Phys.*, **100**, 043907 (2006).
- ³⁹A. V. Nazarov, D. Ménard, J. J. Green, C. E. Patton, G. M. Argentina, and H. J. Van Hook, "Near Theoretical Microwave Loss in Hot Isostatically Pressed (Hipped) Polycrystalline Yttrium Iron Garnet," *J. Appl. Phys.*, **94**, 7227–34 (2003).
- ⁴⁰W. Chen, Y. Kinemuchi, K. Watari, T. Tamura, and K. Miwa, "Preparation of Grain-Oriented $\text{Sr}_{0.3}\text{Ba}_{0.5}\text{Nb}_2\text{O}_6$ Ferroelectric Ceramics by Magnetic Alignment," *J. Am. Ceram. Soc.*, **89**, 381–4 (2006). □